

Al-Ni 复合涂层的结合强度及耐蚀性能研究

王永刚^{1,2}, 刘鑫², 孙亮², 王强¹

(1. 西安建筑科技大学 冶金工程学院, 西安 710055; 2. 中国特种设备检测研究院
特种设备安全与节能国家市场监管重点实验室, 北京 100029)

摘要: **目的** 研究冷喷涂 Al-Ni 复合涂层的结合强度和耐蚀性能, 尝试通过在 Q345R 钢材表面制备防护涂层的方法来改善 Q345R 钢的服役寿命。**方法** 采用冷喷涂技术在 Q345R 板材表面制备纯 Al 涂层和 Al-Ni 复合涂层, 利用 SEM 观察、拉伸试验、腐蚀质量损失试验和 EIS 测试等技术, 测试与分析涂层的结合强度和耐蚀性能, 研究 Ni 粉的含量对涂层的孔隙率、显微组织、涂层-基体间结合强度和耐蚀性能的影响规律。**结果** 涂层与 Q345R 钢结合良好, 在 500 倍电子显微镜下, 界面处没有观察到明显的孔洞与裂纹。由于 Ni 颗粒的夯实作用, Al-Ni 复合涂层的致密性有所提高。相比纯 Al 涂层, Al-10Ni 复合涂层的界面结合强度有略微提升, 断裂失效形式为典型的界面粘结断裂。Al-15Ni 复合涂层的界面结合强度提升明显, 其强度为 31 MPa。腐蚀结果显示, 纯 Al 涂层和 Al-Ni 复合涂层的腐蚀质量损失率较基体材料 Q345R 钢都明显降低, 耐蚀性能有所提升。其中纯 Al 涂层的耐蚀性最好, 腐蚀质量损失率为 0.26 g/(cm²·a), 而 Q345R 基体的腐蚀质量损失率为 2.95 g/(cm²·a)。**结论** 冷喷涂 Al-Ni 复合涂层与基体结合良好, 其耐蚀性优于 Q345R 基体, 可为基体提供保护作用, 其中 Ni 颗粒的质量分数为 15% 时, 涂层的结合强度和耐蚀性综合性能最好。

关键词: 压力容器; Al-Ni 复合涂层; 结合强度; 腐蚀性能

中图分类号: TG174.4 **文献标识码:** A **文章编号:** 1001-3660(2022)07-0176-10

DOI: 10.16490/j.cnki.issn.1001-3660.2022.07.017

Bonding Strength and Corrosion Resistance of Al-Ni Composite Coatings

WANG Yong-gang^{1,2}, LIU Xin², SUN Liang², WANG Qiang¹

(1. School of Metallurgical Engineering, Xi'an University of Architecture and Technology, Xi'an 710055, China;
2. Key Laboratory of Special Equipment Safety and Energy-saving for State Market Regulation, China
Special Equipment Inspection and Research Institute (CSEI), Beijing 100029, China)

ABSTRACT: With the basic equipment of national economic development, pressure vessel is widely used in the sector of petroleum, chemical, energy and other industries. However, due to the complex working environment, the surface of the equipment is easy to generate mechanical scratches, corrosion and wear defects, which affect the service life of the plate. As a

收稿日期: 2021-06-01; 修订日期: 2021-11-17

Received: 2020-06-01; Revised: 2021-11-17

基金项目: 国家重点研发计划 (2016YFC0801905)

Fund: National Key Research Project (2016YFC0801905)

作者简介: 王永刚 (1996—), 男, 硕士研究生, 主要研究方向为冷喷涂技术及应用。

Biography: WANG Yong-gang (1996-), Male, Postgraduate, Research focus: development and application of cold spraying technology.

通讯作者: 刘鑫 (1990—), 男, 博士, 工程师, 主要研究方向为结构完整性评价和冷喷涂技术及应用。

Corresponding author: LIU Xin (1990-), Male, Doctor, Engineer, Research focus: structural integrity evaluation and development and application of cold spraying technology.

引文格式: 王永刚, 刘鑫, 孙亮, 等. Al-Ni 复合涂层的结合强度及耐蚀性能研究[J]. 表面技术, 2022, 51(7): 176-185.

WANG Yong-gang, LIU Xin, SUN Liang, et al. Bonding Strength and Corrosion Resistance of Al-Ni Composite Coatings[J]. Surface Technology, 2022, 51(7): 176-185.

rapid prototyping technology characterized by low temperature and solid deposition of powder, cold spraying technology has been widely used in additive manufacturing, anti-corrosion coating preparation, repair and remanufacturing. In this paper, pure Al coating and Al-Ni composite coating are prepared on the surface of Q345R steel by adding different contents of Ni powder in cold spraying Al powder. The influence of Ni powder particles in terms of the bonding strength and corrosion resistance of the coatings is systematically studied.

Pure Aluminum, Al-10wt.%Ni, Al-15wt.%Ni and Al-20wt.%Ni coatings (The following was called Al coating and Al-10Ni, Al-15Ni, Al-20Ni composite coatings) are prepared by cold spraying on Q345R substrate. The microstructure, porosity, bonding strength and corrosion resistance of the coating are tested by SEM observation, XRD analysis, tensile test, electrochemical test and weight loss test.

The results show that the plastic deformation of Al particles increases and the porosity of the coating decreases due to the tamping of Ni particles. With the increase of Ni particles content, the coating becomes more compact. The porosity of Al coating and Al-10Ni, Al-15Ni, Al-20Ni composite coatings are 5.8%, 1.5%, 1.0% and 0.8%. The bonding strength of Al coating and Al-10Ni, Al-15Ni, Al-20Ni composite coatings are 14.6, 15.2, 31.0 and 22.0 MPa. During the deposition process, the impact of Ni particles makes the interface bonding area between the coating and the substrate become bigger. On the other hand, some Ni particles embedded in the surface of the substrate have a pinning effect on the interface between the coating and the substrate, and these conditions are favorable for increasing the bonding strength. Corrosion weight loss test and electrochemical test are used to evaluate the corrosion resistance of the coating. The conventional three-electrode system is used in the experiment, and the scanning frequency is $0.01\sim 10^5$ Hz. The samples are encapsulated with epoxy resin, and the 3.5% sodium chloride solution is for test. According to the actual application environment of Q345R steel, the solution is added with acetic acid to adjust the pH value to 2.8. It can be found that the corrosion weight loss rates of Q345R steel substrate, pure Al coating, Al-10Ni, Al-15Ni and Al-20Ni composite coatings are 2.95, 0.26, 2.38, 1.32 and 1.34 g/(cm²·a). The corrosion weight loss rate of the four coatings is lower than that of Q345R steel, which indicates that both pure Al coating and Al-Ni composite coating can effectively protect the substrate material. However, compared with pure Al coating, the corrosion weight loss rate of Al-Ni composite coating increases possibly due to the existence of potential difference between Al element and Ni element in Al-Ni composite coating, which is easy to form galvanic corrosion and promotes the corrosion of Al element in the composite coating. Zview software is used to fit the electrochemical test results, and the electrochemical test results are consistent with the conclusion of corrosion weight loss test.

Compared with Q345R substrate, pure Al coating and Al-Ni composite coating have better corrosion resistance, which can effectively prevent the corrosive medium from contacting directly with the substrate and prevent the substrate from being corroded. In practical engineering applications, Q345R steel has high requirements for comprehensive indicators of corrosion resistance and bond strength. This paper systematically compares the bonding strength and corrosion resistance of composite coatings with nickel content of 10%, 15% and 20%. The results show that when nickel content is 15%, the composite coating has the best bonding strength and corrosion resistance, which provides data to evidence the preparation of protective coatings for pressure vessels.

KEY WORDS: pressure vessel; Al-Ni composite coatings; bonding strength; corrosion resistance

冷喷涂技术是一种以粉末低温固态沉积为特点的快速成形技术,在增材制造、防腐涂层制备、修复与再制造等领域有广泛应用^[1]。其工作原理是以压缩气体(氮气、氦气、压缩空气等)为加速介质,带动粉末颗粒在 Laval 喷嘴中加速至超音速,高速运动的喷涂颗粒撞击基体表面后,发生强烈的塑性变形,随后沉积成形^[2],如图 1 所示。与热喷涂、等离子喷涂等喷涂技术相比,冷喷涂技术的最大优势是低温固态成形,可有效避免对粉末颗粒和基体材料的热影响^[3]。

压力容器作为国民经济发展的基础性设备,被广

泛应用于石油、化工、能源等行业中^[4-5]。然而由于工作环境复杂,设备表面易产生机械划痕、腐蚀及磨

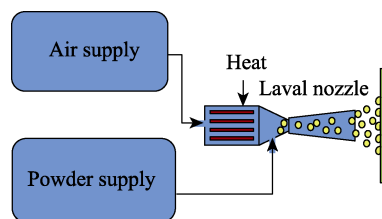


图 1 冷喷涂原理

Fig.1 Principle diagram of cold spray

损等缺陷,影响板材的服役寿命^[6-7]。调查结果显示,在压力容器失效类型中,由于腐蚀导致的失效案例占总体的 80%左右,这直接造成的经济损失约占国家 GDP 的 1.25%~3.5%^[8]。有研究表明,利用冷喷涂技术制备防护涂层是减缓腐蚀的有效解决途径之一^[9]。李相波等^[10]、虞思琦等^[11]在碳钢和镁合金基体上制备了铝基涂层,研究表明,铝涂层具有优良的耐腐蚀性能,可有效地防护基体材料。邱善广等^[12]在碳钢表面制备了铝涂层,通过海水浸泡试验和电化学试验评价了铝涂层的耐蚀性,研究发现,Al 涂层在介质中可以形成致密的氧化膜,具有自钝化作用,可为钢基体提供有效的保护作用。虽然纯 Al 涂层具有良好的耐蚀性能,但其与钢基体的界面结合强度较低。王强等^[13]在 Q345R 钢表面制备了纯 Al 涂层,发现界面结合强度仅有 14.6 MPa,而在实际的工程应用中, Q345R 钢材需要承受一定的载荷,这使得纯 Al 涂层的应用受到了一定的限制。前期有研究发现^[14],在冷

喷涂 Al 粉中加入适量的 Ni 粉,由于 Ni 颗粒在沉积过程中的持续夯实作用,复合涂层的孔隙率、结合强度指标均有所提高,但是对于其耐蚀性能尚未进行研究。因此,为研究 Ni 粉末颗粒加入对涂层耐腐蚀性能的影响规律,本文通过在冷喷涂 Al 粉末中添加不同含量的 Ni 粉末,在 Q345R 钢表面制备了纯 Al 涂层和 Al-Ni 复合涂层,系统地研究了 Ni 粉末颗粒的加入对涂层-基体间结合强度和涂层耐蚀性能的影响。

1 试验

1.1 材料

选用平均粒径为 15 μm 的球形 Al 粉和平均粒径为 30 μm 的类球形 Ni 粉末作为喷涂原材料,粉末形貌和粒径分布如图 2 和图 3 所示。喷涂基体材料为压力容器钢材,牌号为 Q345R,具体的化学成分见表 1。

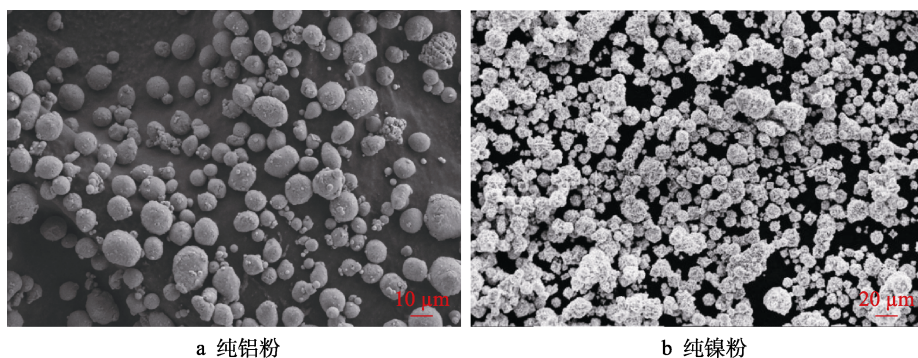


图 2 粉末颗粒的扫描电镜二次电子显微像

Fig.2 Secondary SEM Images of powders: a) pure Al powder; b) pure Ni powder

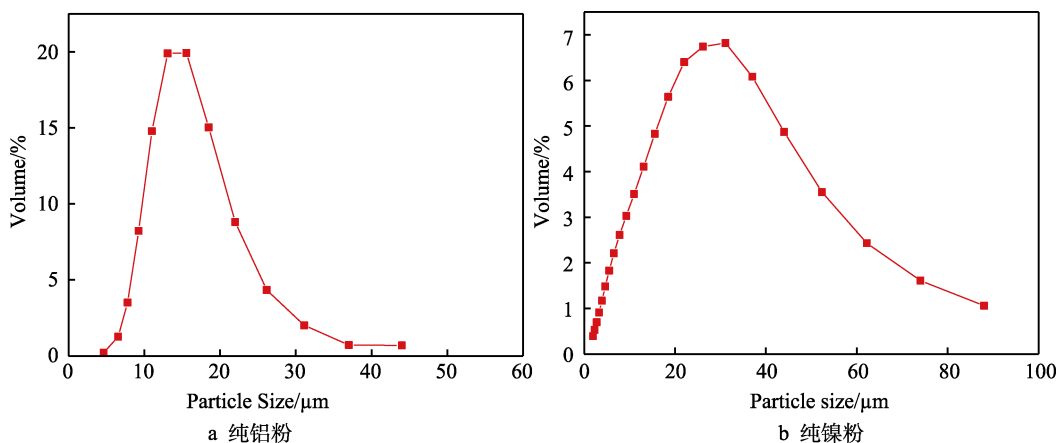


图 3 粉末粒径分布

Fig.3 Particle size distribution: a) pure Al powder; b) pure Ni powder

表 1 Q345R 钢化学成分分析

Tab.1 Chemical composition analysis of Q345R steel

wt. %									
C	Si	Mn	P	S	Al	Ni	Cr	Mo	Fe
0.200	0.550	1.200	0.025	0.010	0.020	0.300	0.300	0.080	Bal.

1.2 预处理

对基体材料和原始粉末做以下处理:为增大基体表面的粗糙度,对基体表面进行喷砂处理;对原始粉末进行配比、混合、干燥处理,最终配制得粉末比例

为纯 Al、Al-10%Ni、Al-15%Ni 和 Al-20%Ni 的混合粉末(后文简称为纯 Al、Al-10Ni、Al-15Ni、Al-20Ni)。采用低压冷喷涂设备制备厚度约为 1~1.5 mm 的 3 种不用 Ni 含量的涂层,工作气体为高纯度的 N₂,具体的参数见表 2。将制备好的样品进行切割、镶样、打磨和抛光处理,最后在显微镜下观察。

表 2 喷涂工艺参数
Tab.2 The process parameters of cold spraying

Gas pressure/MPa	Gas temperature/℃	Adjacent spraying path distance/mm	Stand-off distance/mm	Nozzle move rate/(mm·s ⁻¹)	Cycles
1	300	1	12	30	4

1.3 方法

采用 SEM 观测涂层与界面的微观形貌,在 50×、500×电子显微镜下分析粉末颗粒的变形和界面结合状态。采用 Image Pro 软件,利用面积比法统计涂层的孔隙率,在 1000×电子显微镜下对每个样品拍摄 8 张 SEM 照片,分别对每一张照片进行孔隙率统计,最后求取平均值。根据 ASTM C633^[15],采用拉伸试验测量结合强度,每组样品设定 3 个平行拉伸样,最后求取平均值。采用 X 射线衍射仪分析纯 Al 涂层和 Al-Ni 复合涂层的物相结构,利用 Jade 软件分析 XRD 图谱。

采用腐蚀质量损失试验和电化学测试技术来评价涂层的耐蚀性,每组样品均设定 3 个平行试样,腐

蚀质量损失试样采用硅胶对其他 5 个没有涂层的表面进行封装,试验温度为 35 ℃,试验时间为 72 h。采用 Gamry 电化学工作站测量电化学阻抗谱,试验采用常规的三电极体系,扫描频率为 0.01~10⁵ Hz。试样采用环氧树脂进行封装,试验溶液均为 3.5%氯化钠溶液。根据 Q345R 钢的实际应用环境,加醋酸将溶液 pH 值调节为 2.8。

2 结果与讨论

2.1 显微组织

不同倍数下涂层与基体界面的背散射 SEM 形貌如图 4 所示。由图 4a 可见,纯 Al 涂层平均厚度约为

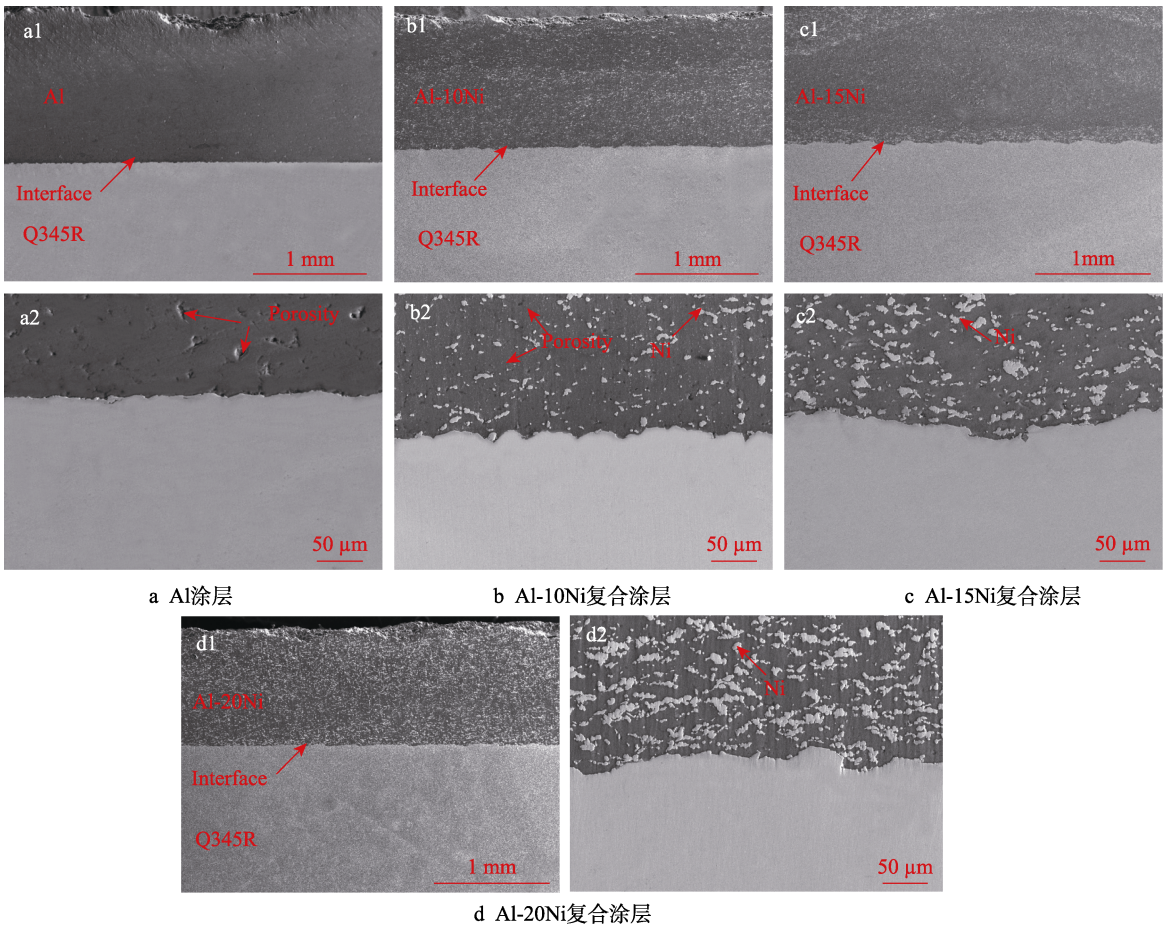


图 4 涂层截面的 SEM 形貌

Fig.4 The cross-sectional SEM images of cold sprayed coating: a) Al coating; b) Al-10Ni composite coating; c) Al-15Ni composite coating; d) Al-20Ni composite coating

1.5 mm。从图 4a2 中可以看出,涂层与基体界面处结合良好,但在涂层内部存在一定的孔隙(孔隙率为 5.8%)。这是因为在喷涂过程中,部分 Al 粉末颗粒之间塑性变形不充分。由图 4b1、c1、d1 可见,Al-Ni 复合涂层的平均厚度约为 1 mm,可以看出 Ni 粉末颗粒在涂层中均匀分布,其中白色部分为 Ni 颗粒,暗色部分为 Al 颗粒。观察图 4b2、c2、d2 可以看出,加入 Ni 粉末之后,涂层内部的孔隙明显减少。经统计,Al-10Ni 涂层的孔隙率为 1.5%,Al-15Ni 涂层的孔隙率为 1.0%,Al-20Ni 涂层的孔隙率为 0.8%。孔隙率的降低一方面归结于 Ni 粉末在沉积过程中起

到的夯实作用,提高了 Al 粉末颗粒间的塑性变形程度,使涂层更加致密^[16-17];另一方面,Ni 粉末颗粒在涂层中起到增强相的作用。另外,在涂层与基体的界面处存在少量的 Ni 颗粒,这也有助于增加涂层与基体的界面结合面积^[18],提高涂层/基体间的咬合力。

纯 Al 涂层和 Al-Ni 复合涂层的物相分析如图 5 所示。可以看出,在纯 Al 涂层中仅有 Al 相,Al-Ni 复合涂层中只有 Al 相和 Ni 相两种相结构,未发现其他相成分。这说明粉末颗粒在沉积过程中,并未发生氧化,而是保持着原始粉末的相结构。

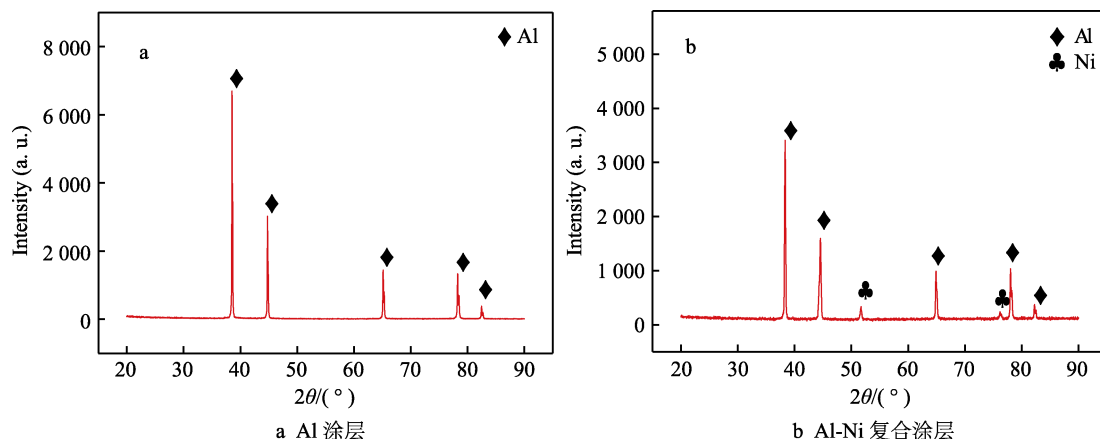


图 5 纯 Al 涂层和 Al-Ni 复合涂层的 XRD 图

Fig.5 The XRD diagram of pure Al coating and Al-Ni composite coatings: a) Al coating; b) Al-Ni composite coatings

2.2 结合强度

纯 Al 和 Al-Ni 复合涂层的结合强度测试结果如图 6 所示。其中纯 Al、Al-10Ni、Al-15Ni 和 Al-20Ni 涂层与基体的界面结合强度分别为 14.6、15.2、31.0、22.0 MPa,计算公式见式(1)。当增加 Ni 颗粒之后,涂层与基体的界面结合强度有所提升,原因在于喷涂颗粒在沉积过程中,Ni 颗粒的撞击一方面增大了涂层与基体间的界面结合面积;另一方面,部分 Ni 颗粒嵌入到基体表层后,对涂层/基体界面处有钉扎作用,见图 4b2、c2、d2 界面处。这些基体表层存在的

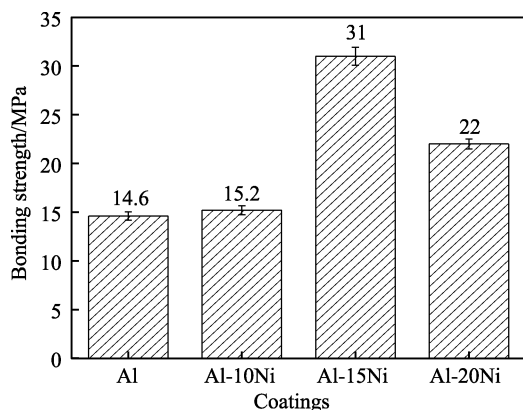


图 6 涂层结合强度

Fig.6 The bond strength of coating

Ni 颗粒一定程度上提高了界面结合强度^[19-20]。

$$\sigma = \frac{F}{S} \quad (1)$$

前期研究表明,拉伸试样涂层断裂失效的方式通常有 3 种形式,分别为涂层内部断裂(Cohesion strength)、涂层与基体界面断裂(Adhesion strength)、复合断裂模式^[21]。纯 Al 涂层的宏观断裂形貌如图 7a 所示,可以看出,在基体一侧的表面上仅有少量的 Al 涂层颗粒的残留,因此断裂方式为界面粘结断裂。图 7b、c、d 为 Al-Ni 复合涂层的宏观断裂形貌,可以看出,在基体一侧的表面上有明显的涂层残留,在侧涂层内部产生明显的撕裂,可认为失效形式是以界面粘着断裂为主、涂层内部粘聚断裂为辅的复合失效模式^[22]。

2.3 腐蚀试验

2.3.1 质量损失试验

涂层与基体在 pH=2.8 的 NaCl 溶液中的腐蚀质量损失率的变化如图 8 所示。可以看出,Q345R 钢基体、纯 Al 涂层、Al-10Ni、Al-15Ni 和 Al-20Ni 复合涂层的腐蚀质量损失率分别为 2.95、0.26、2.38、1.32、1.34 g/(cm²·a)。4 种涂层的腐蚀质量损失率均低于 Q345R 钢基体,这说明纯 Al 涂层和 Al-Ni 复合涂层均可有效地保护基体材料。相比纯 Al 涂层,Al-Ni 复合涂层的腐蚀质量损失率有所增大,这可能是由于

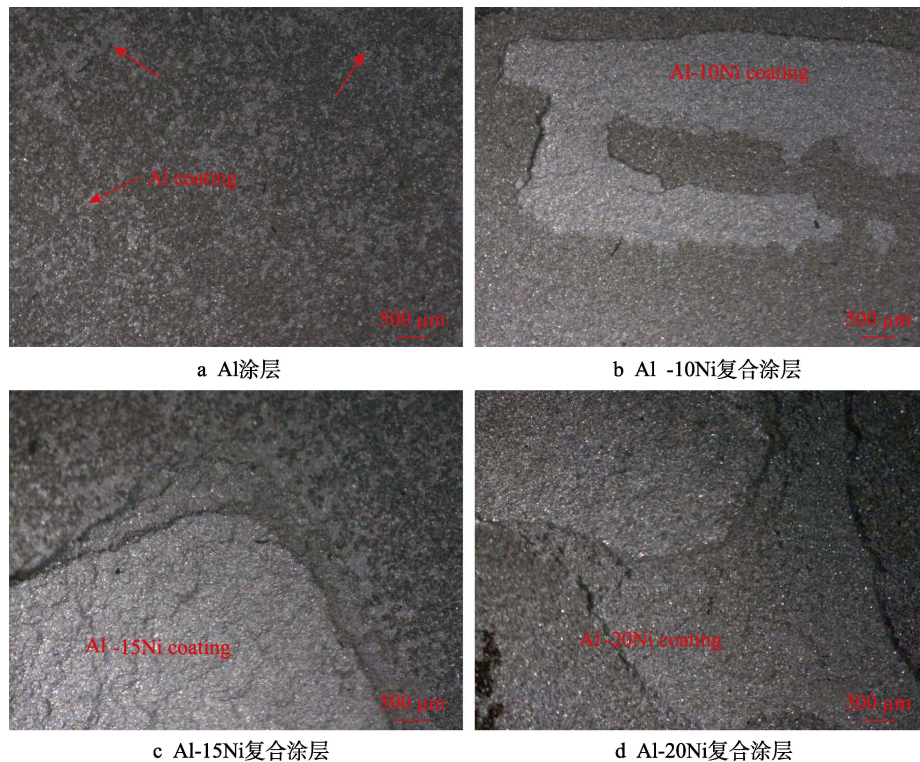


图 7 基体侧涂层宏观断口形貌

Fig.7 The morphology of fracture surface in coating: a) Al coating; b) Al-10Ni composite coating; c) Al-15Ni composite coating; d) Al-20Ni composite coating

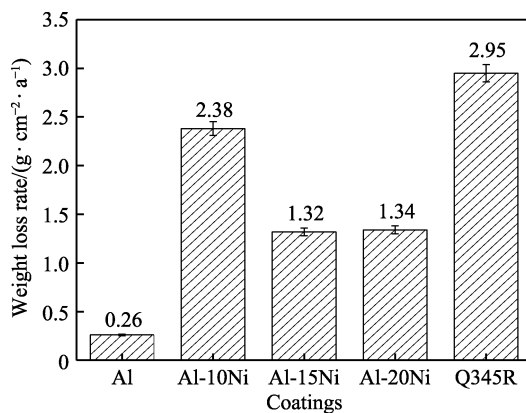
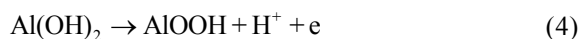
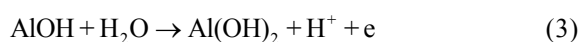
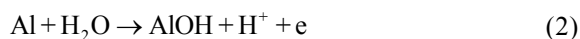


图 8 涂层和基体的腐蚀质量损失率

Fig.8 Corrosion weight loss rate of coatings and substrate

Al-Ni 复合涂层中 Al 元素和 Ni 元素之间存在着电位差, 易形成电偶腐蚀, 对复合涂层中 Al 元素的腐蚀有促进作用。

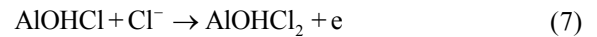
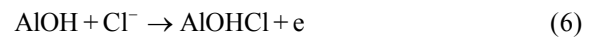
通常情况下, Al 涂层在 NaCl 水溶液中会氧化形成钝化膜 $\text{Al}_2\text{O}_3 \cdot \text{H}_2\text{O}$, 反应式如下:



总反应式为:



由于 NaCl 水溶液中存在着活性 Cl^- , 因此在反应 (2) 之后发生以下反应:



另外, 与 Al-10Ni 复合涂层相比, Al-15Ni 和 Al-20Ni 复合涂层的质量损失现象有所降低, 涂层的耐蚀性更好。这是因为在涂层的覆盖屏蔽作用下, 腐蚀介质难以渗入到基体材料表面, 从而延缓了基体材料的腐蚀, 因此耐蚀性与复合涂层的孔隙率密切相关, 而 Al-10Ni 复合涂层的孔隙率高, 腐蚀介质就越易渗入进涂层内部, 因此耐蚀性就越差。另一方面可能与涂层的腐蚀类型相关。如图 9 所示, Al-10Ni 涂层以均匀的面腐蚀为主, 而 Al-20Ni 涂层以局部腐蚀 (点蚀) 为主。由于复合涂层中随着 Ni 的占比增加, 涂层表面不易形成氧化膜, 而介质中活性阴离子 Cl^- 的半径较小, 容易穿过涂层表面, 使得涂层局部破坏出现点蚀坑^[23-24]。

2.3.2 电化学测试

电化学阻抗谱 (Electrochemical Impedance Spectroscopy) 作为电化学测试中评价材料耐蚀性的重要指标, 主要研究交流阻抗随频率的变化关系^[25]。拟合的等效电路如图 10 所示, 其中 Q345R 基体的 EIS 阻抗谱用 $R_s[Q_c(R_cW)]$ 模型拟合 (见图 10a); 涂层的 EIS 阻抗谱用 $R_s\{Q_c[R_c(R_{ct}Q_{dl})(R_L L)]\}$ 模型拟合 (见图 10b)。 R_s 表示 3.5%NaCl 溶液的电阻; R_c 为涂层表面氧化膜电阻; Q_c 表示电容 CPE ($0.5 < n < 1$); R_{ct} 表示

电荷转移电阻; Q_{dl} 表示双电层电容 CPE ($0.5 < n < 1$); L 和 R_L 表示感抗和感抗电阻; W 表示扩散引起的韦伯阻抗, 各元件的拟合参数见表 3。可以看出, Q345R 基体的 R_c 仅为 $270 \Omega \cdot \text{cm}^2$ 。因此, 在腐蚀介质中, 氧

化膜的保护作用很小, 而 Al-Ni 复合涂层的 R_c 较大, 说明氧化膜的保护作用增强, 耐蚀性有所增大。相比之下, 纯 Al 涂层的 R_c 为 $2 \times 10^3 \Omega \cdot \text{cm}^2$, 表面致密的氧化膜在腐蚀介质中表现出更优异的耐蚀性。

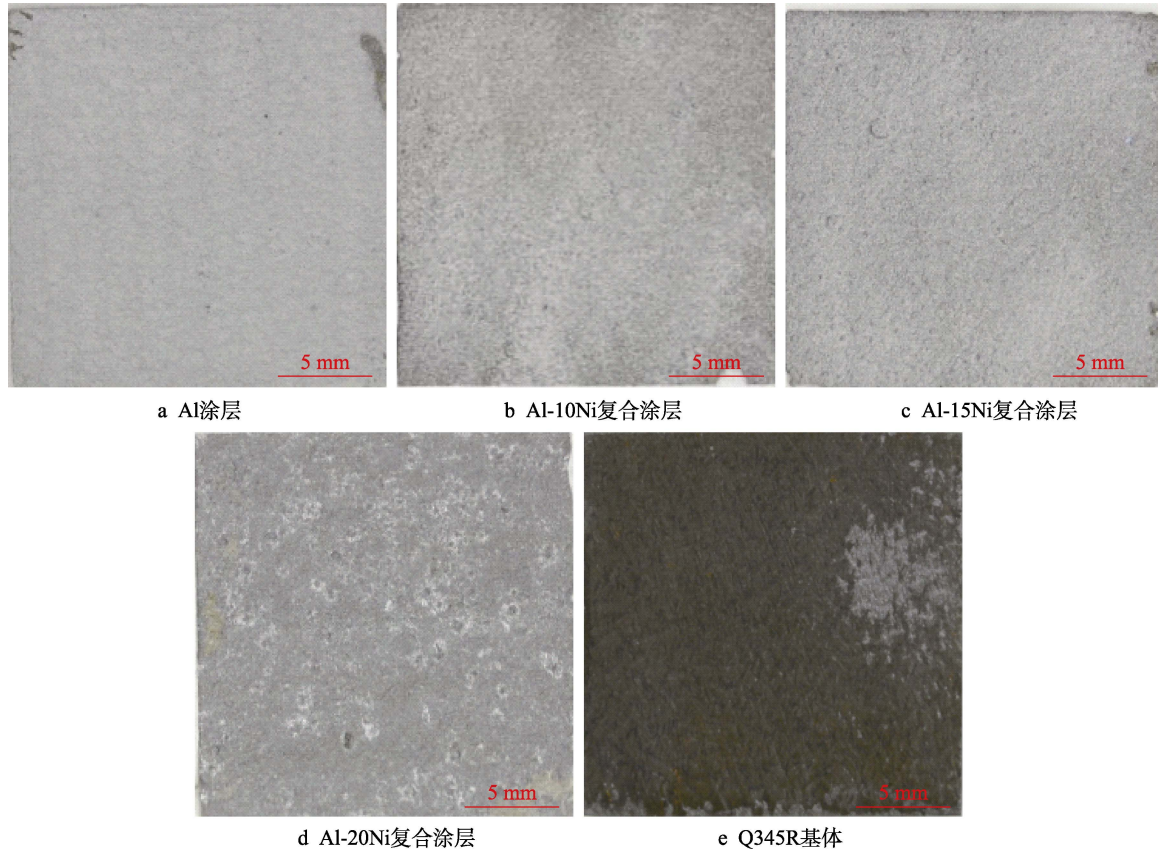


图 9 浸泡腐蚀形貌宏观

Fig.9 The morphology of immersion corrosion: a) Al coating; b) Al-10Ni composite coating; c) Al-15Ni composite coating; d) Al-20Ni composite coating; e) Q345R substrate

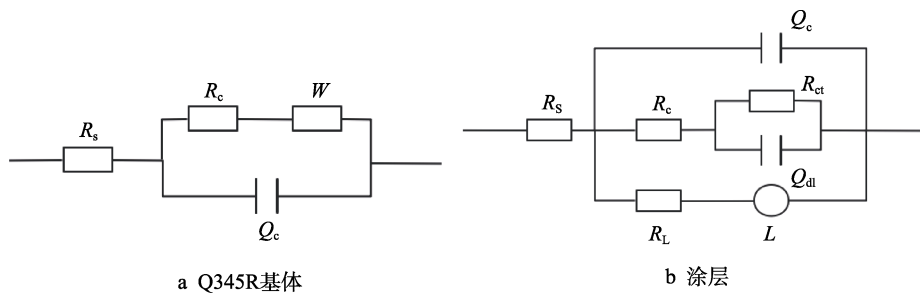


图 10 拟合的试验数据等效电路

Fig.10 Electrical equivalent circuit for fitting the experimental data: a) Q345R substrate; b) coatings

表 3 涂层与基体的 EIS 拟合参数

Tab.3 Fitted EIS parameters for the coatings and substrate

Sample	$R_s/(\Omega \cdot \text{cm}^2)$	$Q_c/(\text{F} \cdot \text{cm}^2)$	n_1	$R_c/(\Omega \cdot \text{cm}^2)$	$Q_{dl}/(\text{F} \cdot \text{cm}^2)$	n_2	$R_{ct}/(\Omega \cdot \text{cm}^2)$	$R_L/(\Omega \cdot \text{cm}^2)$	$L/(\text{H} \cdot \text{cm}^2)$
Q345R	5.94	1.65×10^{-4}	0.78	269	—	—	—	—	—
Pure Al coating	7.23	5.04×10^{-4}	0.64	2 000	1.1×10^{-4}	0.6	200	550	1 000
Al-10Ni composite coating	9.04	5.62×10^{-5}	0.77	680	2.36×10^{-5}	0.77	168	550	842
Al-15Ni composite coating	10.23	5.54×10^{-5}	0.76	760	2.36×10^{-5}	0.77	168	550	860
Al-20Ni composite coating	9.79	5.5×10^{-5}	0.76	730	2.36×10^{-5}	0.77	168	550	840

从图 11a1 可以看出, Q345R 的阻抗弧特征主要表现为中高频的容抗弧和低频的直线特征。这是因为在中高频界面, 双电层电容 Q_c 主要通过电荷传递过程控制, 而在低频阶段, 双电层电容 Q_c 由扩散控制。纯 Al 涂层和 Al-Ni 复合涂层则表现为中高频的容抗弧和低频的感抗弧特征, 见图 11a2。不难看出, 4 种涂层的容抗弧半径均大于 Q345R 基体, 这说明相对基体材料, 涂层的耐蚀性能更好。从图 11 中还可以看出, 纯 Al 涂层的容抗弧半径远大于 Al-Ni 复合涂层, 表现出更好的耐蚀性, 原因在于纯 Al 涂层表面更易形成致密的钝化膜, 能有效地阻止腐蚀介质的渗

入过程^[26-27]。

图 11b 为涂层与基体的 Bode 图, 前期研究发现, 低频阻抗模值的大小往往与耐蚀性相关, 低频的阻抗值越大, 则耐蚀性能越好^[28]。从图 11b2 可以看出, 在低频阶段 (0.01~1 Hz), 相比基体材料, 冷喷涂涂层均表现出较好的耐蚀性。基体与材料的极化曲线如图 12 所示, 经过外推法拟合纯 Al、Al-10Ni、Al-15Ni 和 Al-20Ni 涂层与基体 Q345R 的腐蚀电流密度分别为: 9.1×10^{-6} 、 3.0×10^{-5} 、 2.2×10^{-5} 、 2.9×10^{-5} 、 5.8×10^{-5} A/cm²。这与 2.3.1 中腐蚀质量损失试验的结论保持一致, 说明涂层能对基体提供一定程度的保护作用^[29]。

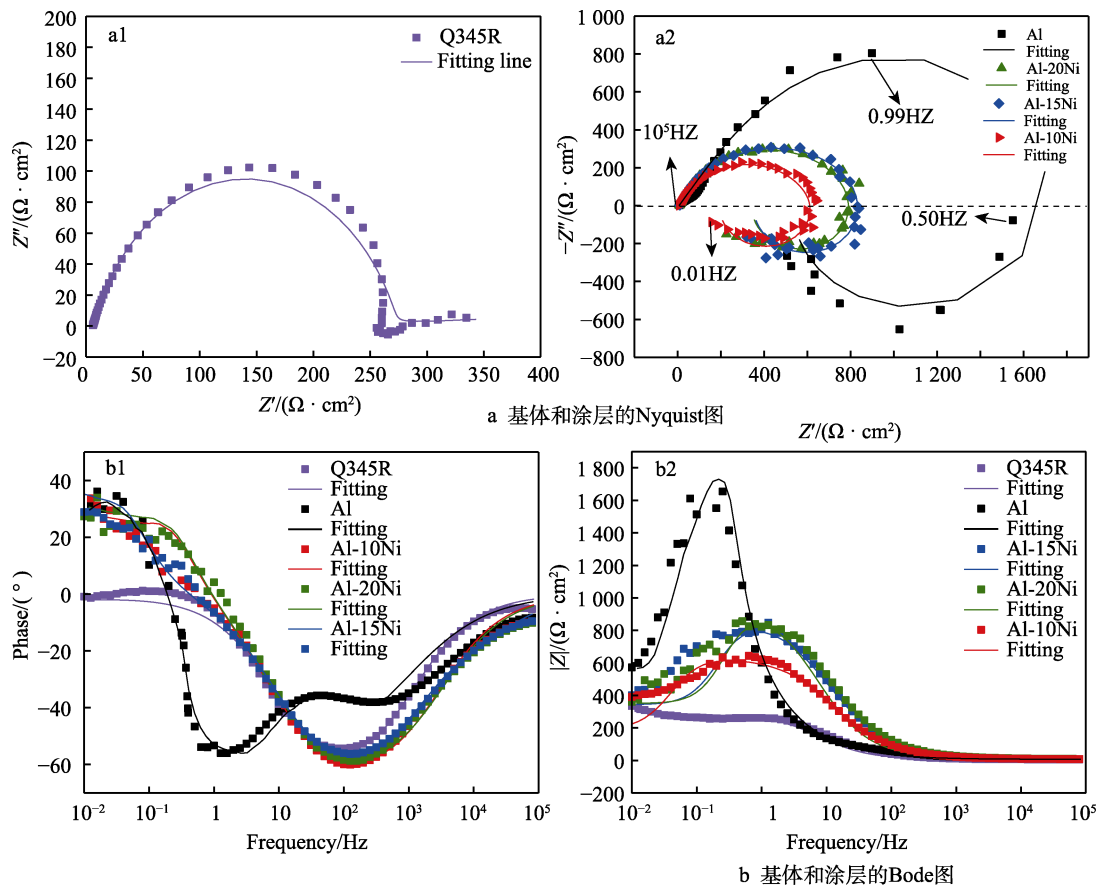


图 11 涂层与基体在 3.5% NaCl 溶液中的 Nyquist 和 Bode 图

Fig.11 The Nyquist and Bode pictures of the coatings and substrate in a 3.5% NaCl solution:

a) Nyquist pictures; b) Bode pictures

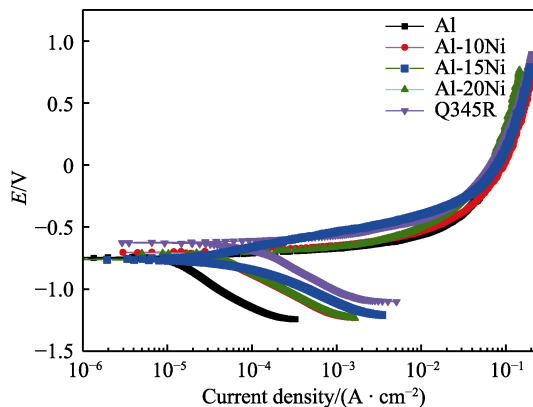


图 12 涂层与基体的极化曲线

Fig.12 Polarization curves of substrate and coatings

3 结论

1) Ni 颗粒的加入一方面在涂层/基体界面处起到了钉扎作用, 另一方面增大了涂层/基体间的结合面积, 提升了界面结合强度。

2) 与 Q345R 基体相比, 纯 Al 涂层和 Al-Ni 复合涂层有更好的耐蚀性, 可有效地阻止腐蚀介质与基体直接接触, 防止基体受到腐蚀。

3) 对比镍添加量为 10%、15%、20%复合涂层的结合强度和耐蚀性, 结果表明, 当镍添加量为 15% 时, 复合涂层的结合强度和耐蚀性能综合最优。

参考文献:

- [1] 李文亚, 曹聪聪, 杨夏炜, 等. 冷喷涂复合加工制造技术及其应用[J]. 材料工程, 2019, 47(11): 53-63.
LI Wen-ya, CAO Cong-cong, YANG Xia-wei, et al. Cold Spraying Hybrid Processing Technology and Its Application[J]. Journal of Materials Engineering, 2019, 47(11): 53-63.
- [2] YIN Shuo, CAVALIERE P, ALDWELL B, et al. Cold Spray Additive Manufacturing and Repair: Fundamentals and Applications[J]. Additive Manufacturing, 2018, 21: 628-650.
- [3] 李文亚, 张冬冬, 黄春杰, 等. 冷喷涂技术在增材制造和修复再制造领域的应用研究现状[J]. 焊接, 2016(4): 2-8.
LI Wen-ya, ZHANG Dong-dong, HUANG Chun-jie, et al. State of the Art of Cold Spraying Additive Manufacturing and Remanufacturing[J]. Welding & Joining, 2016(4): 2-8.
- [4] 张贤安, 郑三龙. Q345R 钢厚板焊接接头断裂疲劳性能试验研究[J]. 石油化工设备, 2014, 43(1): 17-22.
ZHANG Xia-nan, ZHENG San-long. Experimental Study in Fracture and Fatigue Property of Weld Jointing with Thick Q345R Steel Plate[J]. Petro-Chemical Equipment, 2014, 43(1): 17-22.
- [5] 孙长玉, 霍培珍. Q345R 锅炉压力容器钢板的研制[J]. 包钢科技, 2015, 41(3): 39-41.
SUN Chang-yu, HUO Pei-zhen. Development of Pressure Vessel Steel Plate Q345R for Boiler[J]. Science & Technology of Baotou Steel, 2015, 41(3): 39-41.
- [6] 殷金泉, 程强强, 于润桥. 基于扩展有限元的 Q345R 材料平板裂纹扩展模拟研究[J]. 失效分析与预防, 2019, 14(6): 361-365.
YIN Jin-quan, CHENG Qiang-qiang, YU Run-qiao. Simulation Study on Crack Propagation of Q345R Material Based on Extended Finite Element Method[J]. Failure Analysis and Prevention, 2019, 14(6): 361-365.
- [7] DAI Hai-long, SHI Shou-wen, GUO Can, et al. Pits Formation and Stress Corrosion Cracking Behavior of Q345R in Hydrofluoric Acid[J]. Corrosion Science, 2020, 166: 108443.
- [8] 张玉福. 多介质环境下压力容器用材腐蚀失效机理研究[D]. 兰州: 兰州理工大学, 2016.
ZHANG Yu-fu. The Research on the Corrosion Failure Mechanism of Pressure Vessel Materials under Multi-Media Environment[D]. Lanzhou: Lanzhou University of Technology, 2016.
- [9] 张宇婷, 朱国强, 崔美红. 表面处理技术的种类和发展[J]. 化工管理, 2019(31): 4-5.
ZHANG Yu-ting, ZHU Guo-qiang, CUI Fu-hong. Types and Development of Surface Treatment Technologies[J]. Chemical Enterprise Management, 2019(31): 4-5.
- [10] 李相波, 许立坤, 邱善广, 等. 碳钢低压冷喷涂铝涂层的海水耐腐蚀性[J]. 电化学, 2013, 19(5): 425-429.
LI Xiang-bo, XU Li-kun, QIU Shan-guang, et al. Corrosion Resistance of Low Pressure Cold Sprayed Al Coating on Q235 Steel in Seawater[J]. Journal of Electrochemistry, 2013, 19(5): 425-429.
- [11] 虞思琦, 杨夏炜, 李文亚, 等. 镁合金表面冷喷涂铝合金与铝基复合涂层组织和耐蚀性研究[J]. 上海航天, 2018, 35(4): 101-107.
YU Si-qi, YANG Xia-wei, LI Wen-ya, et al. Microstructure and Corrosion Behavior of Cold Sprayed Aluminum Alloy and Aluminum Matrix Composite Coatings on Magnesium Alloy[J]. Aerospace Shanghai, 2018, 35(4): 101-107.
- [12] 邱善广. 低压冷喷涂铝涂层的防腐性能研究[D]. 青岛: 中国海洋大学, 2013.
QIU Shan-guang. Research of Anti-Corrosion of Al Coatings by Low Pressure Cold Spray Technology[D]. Qingdao: Ocean University of China, 2013.
- [13] 王强, 王永刚, 牛文娟, 等. Q345R 板材表面冷喷涂 Al-Zn 涂层的组织及性能研究[J]. 表面技术, 2021, 50(2): 287-293.
WANG Qiang, WANG Yong-gang, NIU Wen-juan, et al. Study on the Structure and Properties of Cold Sprayed Al-Zn Composite Coatings on Q345R Plate[J]. Surface Technology, 2021, 50(2): 287-293.
- [14] 李旭, 王强, 杨驹, 等. 原位金属间化合物对冷喷涂 Al-Ni 增材沉积体力学性能的影响[J]. 表面技术, 2020, 49(10): 294-302.
LI Xu, WANG Qiang, YANG Ju, et al. Effect of In-Situ Intermetallic Compounds on Mechanical Properties of Al-Ni Deposits by Cold Spraying[J]. Surface Technology, 2020, 49(10): 294-302.
- [15] HAN W, RYBICKI E F, SHADLEY J R. An Improved Specimen Geometry for ASTM C633-79 to Estimate Bond Strengths of Thermal Spray Coatings[J]. Journal of Thermal Spray Technology, 1993, 2(2): 145-150.
- [16] MEYDANOGLU O, JODOIN B, KAYALI E S. Microstructure, Mechanical Properties and Corrosion Performance of 7075 Al Matrix Ceramic Particle Reinforced Composite Coatings Produced by the Cold Gas Dynamic Spraying Process[J]. Surface and Coatings Technology, 2013, 235: 108-116.
- [17] WINNICKI M, MALACHOWSKA A, PIWOWARCZYK T, et al. The Bond Strength of Al + Al₂O₃ Cermet Coatings Deposited by Low-Pressure Cold Spraying[J]. Archives of Civil and Mechanical Engineering, 2016, 16(4): 743-752.
- [18] 王佳杰, 魏尊杰, 霍树斌, 王吉孝, 张颖, 王志平. 超音速冷气动力喷涂 Cu 涂层的结合机理[J]. 焊接, 2005(9): 36-39.
WANG Jia-jie, WEI Zun-jie, HUO Shu-bin, et al. Bonding Mechanism of Cu Coating by Supersonic Cold Gas Dynamic Spray[J]. Welding & Joining, 2005(9): 36-39.
- [19] ZHANG Zhi-chao, LIU Fu-chun, HAN En-hou, et al. Effects of Al₂O₃ on the Microstructures and Corrosion

- Behavior of Low-Pressure Cold Gas Sprayed Al_{2024} - Al_2O_3 Composite Coatings on AA 2024-T3 Substrate[J]. *Surface and Coatings Technology*, 2019, 370: 53-68.
- [20] IRISSOU E, LEGOUX J G, ARSENAULT B, et al. Investigation of Al- Al_2O_3 Cold Spray Coating Formation and Properties[J]. *Journal of Thermal Spray Technology*, 2007, 16(5/6): 661-668.
- [21] XIONG Yu-ming, ZHUANG W, ZHANG Ming-xing. Effect of the Thickness of Cold Sprayed Aluminium Alloy Coating on the Adhesive Bond Strength with an Aluminium Alloy Substrate[J]. *Surface and Coatings Technology*, 2015, 270: 259-265.
- [22] WANG Qiang, SPENCER K, BIRBILIS N, et al. The Influence of Ceramic Particles on Bond Strength of Cold Spray Composite Coatings on AZ91 Alloy Substrate[J]. *Surface and Coatings Technology*, 2010, 205(1): 50-56.
- [23] 赵麦群, 雷阿丽. 金属的腐蚀与防护[M]. 北京: 国防工业出版社, 2002.
- ZHAO Mai-qun, LEI A-li. *Corrosion and Protection of Metals*[M]. Beijing: National Defense Industry Press, 2002.
- [24] 黄永昌. 金属腐蚀与防护原理[M]. 上海: 上海交通大学出版社, 1989.
- HUANG Yong-chang. *Metal Corrosion and Protection Principle*[M]. Shanghai: Shanghai Jiao Tong University Press, 1989.
- [25] 吴静. 涂层缺陷对铁基非晶合金涂层腐蚀行为影响研究[D]. 合肥: 中国科学技术大学, 2020.
- WU Jing. *Role of Coating Defects in Corrosion Behavior of Fe-Based Amorphous Metallic Coatings*[D]. Hefei: University of Science and Technology of China, 2020.
- [26] 巫业栋, 杨英, 张世宏, 等. Ni 含量对 NiCrN 涂层腐蚀磨损机理的影响[J]. *中国表面工程*, 2019, 32(6): 63-72.
- WU Ye-dong, YANG Ying, ZHANG Shi-hong, et al. Effects of Ni Content on Corrosive Wear Mechanism for NiCrN Coatings[J]. *China Surface Engineering*, 2019, 32(6): 63-72.
- [27] 程丹. Q235 低碳钢表面锌镍复合涂层的腐蚀行为研究[D]. 哈尔滨: 哈尔滨工业大学, 2018.
- CHENG Dan. *Study on the Corrosion Behavior of Zinc-Nickel Composite Coating on Q235 Low Carbon Steel*[D]. Harbin: Harbin Institute of Technology, 2018.
- [28] GANBORENA L, VEGA J M, ÖZKAYA B, et al. AN SKP and EIS Study of Microporous Nickel-Chromium Coatings in Copper Containing Electrolytes[J]. *Electrochimica Acta*, 2019, 318: 683-694.
- [29] 娄昆鹏. 冷喷涂 Al 复合涂层的组织结构与腐蚀行为的研究[D]. 厦门: 集美大学, 2017.
- LOU Kun-peng. *The Organizational Structure of the Cold Spraying Al Composite Coating and Corrosion Behavior Research*[D]. Xiamen: Jimei University, 2017.

责任编辑: 刘世忠

(上接第 175 页)

- [18] CHEN Chun-lin, HE Yi, XIAO Guo-qing, et al. Synergistic Effect of Graphene Oxide@phosphate-Intercalated Hydroxide for Improved Anti-Corrosion and Self-Healable Protection of Waterborne Epoxy Coating in Salt Environments[J]. *Journal of Materials Chemistry C*, 2019, 7(8): 2318-2326.
- [19] JAVIDPARVAR A A, NADERI R, RAMEZANZADEH B. Epoxy-Polyamide Nanocomposite Coating with Graphene Oxide as Cerium Nanocontainer Generating Effective Dual Active/Barrier Corrosion Protection[J]. *Composites Part B: Engineering*, 2019, 172: 363-375.
- [20] MO Qiu-feng, LI Wei-zhou, YANG Hai-juan, et al. Water Resistance and Corrosion Protection Properties of Waterborne Polyurethane Coating Enhanced by Montmorillonite Modified with Ce^{3+} [J]. *Progress in Organic Coatings*, 2019, 136: 105213.
- [21] ZHOU Xing-nan, HUANG Hao-wei, ZHU Rui, et al. Facile Modification of Graphene Oxide with Lysine for Improving Anti-Corrosion Performances of Water-Borne Epoxy Coatings[J]. *Progress in Organic Coatings*, 2019, 136: 105200.
- [22] HILL A J, THORNTON A W, HANNINK R H J, et al. Role of Free Volume in Molecular Mobility and Performance of Glassy Polymers for Corrosion-Protective Coatings[J]. *Corrosion Engineering, Science and Technology*, 2020, 55(2): 145-158.
- [23] NASCIMENTO E D, RAMOS A, WINDMOLLER D, et al. Breakdown, Free-Volume and Dielectric Behavior of the Nanodielectric Coatings Based on Epoxy/Metal Oxides[J]. *Journal of Materials Science: Materials in Electronics*, 2016, 27(9): 9240-9254.
- [24] WU Yang-min, ZHAO Wen-jie, QIANG Yu-jie, et al. π - π Interaction between Fluorinated Reduced Graphene Oxide and Acridizinium Ionic Liquid: Synthesis and Anti-Corrosion Application[J]. *Carbon*, 2020, 159: 292-302.
- [25] RAMEZANZADEH M, RAMEZANZADEH B, SARI M G, et al. Corrosion Resistance of Epoxy Coating on Mild Steel through Polyamidoamine Dendrimer-Covalently Functionalized Graphene Oxide Nanosheets[J]. *Journal of Industrial and Engineering Chemistry*, 2020, 82: 290-302.
- [26] TIAN Yu-qin, XIE Yu-hui, DAI Fei, et al. Ammonium-Grafted Graphene Oxide for Enhanced Corrosion Resistance of Waterborne Epoxy Coatings[J]. *Surface and Coatings Technology*, 2020, 383: 125227.

责任编辑: 万长清